Semiconductor Physics, Quantum Electronics & Optoelectronics, 2020. V. 23, No 2. P. 180-185.

Optics

Magneto-optical properties of nanocomposites $(Co_{41}Fe_{39}B_{20})_x(SiO_2)_{100-x}$

V.O. Lysiuk[1], S.G. Rozouvan[2], V.S. Staschuk[2], V.V. Stukalenko[2]

[1]V. Lashkaryov Institute of Semiconductor Physics, NAS of Ukraine,
41, prospect Nauky, 03680 Kyiv, Ukraine
[2]Taras Shevchenko National University of Kyiv, Faculty of Physics,
64/13 Volodymyrska str., 01601 Kyiv, Ukraine
E-mail: sgr@univ.kiev.ua; svs@univ.kiev.ua; stu@univ.kiev.ua

Abstract. Magneto-optics properties of $(Co_{41}Fe_{39}B_{20})_x(SiO_2)_{100-x}$ alloys were studied applying both experimental spectral ellipsometry and quantum mechanical theory (incl. molecular calculus) approaches. Magneto-optics (MO) properties of the alloys were derived from the measured parameters of reflected elliptically polarized light. The experimental data were explained applying selection rules for the magnetic quantum number. Theoretical approach based on electron gas in a metal with angular momentum coupled to magnetic field demonstrated applicability of the magnetic quantum number and Hund's rule for ascertaining the MO alloys properties. In this modeling, the magneto-optics properties of ferromagnetic alloys can be explained being based on derivations for the magnetic quantum number selection rules. Hund's rule directly influences the dielectric tensor off-diagonal elements signs. The nonrelativistic Schrödinger equation for the Co_2Fe_2B alloy was numerically solved taking into account spins of Co and Fe atoms as well as orbital moments of wave functions in order to check the theoretical approach. As a result, the MO dispersion curves can be theoretically evaluated using the modified Spicer ratio that includes density of states functions with specific azimuthal and spin quantum numbers.

Keywords: cobalt iron boron alloy, modified Spicer ratio, molecular calculus, Hund's rule.

https://doi.org/10.15407/spqeo23.02.180
PACS 75.50.Tt, 78.20.Ls

Manuscript received 14.11.19; revised version received 27.03.19; accepted for publication 10.06.20; published online 12.06.20.

1. Introduction

By cause of modern nanotechnologies, a number of nanoscale magnetic materials has been created, some of which are characterized by gigantic values of magnetoresistance and quantum anomalous Hall effect [1].

These materials are increasingly used in a number of highly novel devices due to this progress.

This applies particularly highly sensitive temperature and magnetic field sensors used both as protective coatings and materials characterized by unique magnetic properties. The range of these properties is significantly expanded, when using a new class of materials – nanocomposites that are two-phase systems consisting of nanogranules of amorphous ferromagnetic materials embedded into a dielectric matrix. Among these, promising are nanocomposites $(Co_{41}Fe_{39}B_{20})_x(SiO_2)_{100-x}$, where x varies discretely from small values close to 10% up to 100%. These systems are characterized by particular (specific) electrical properties, and at certain values of x there occurs a phenomenon of percolation – the hopping mechanism of electric current flow in the sample with high electrical resistivity and abnormal magnetic properties. These systems have found practical application in devices of information storage. It is well known [2] that, in the area of high frequencies, the use of nanostructures becomes more complicated due to the increase of losses caused by eddies currents as the frequency increases, so just the use of nanocomposites at concentrations close to the percolation threshold minimize these losses.

The values of magnetic permeability inherent to the composites are significantly reduced at higher concentrations followed by sharply dropped conductivity, *i.e.*, the material becomes non-conductive. In addition, such structural parameter as the size of granules, or rather, the distribution function of nanogranules by size becomes very essential. It is also important to know the nanogranule structure, including their electronic and phase composition. Structural studies must include optical properties as an important component of electronic properties examination [3].

Supplementing these results with studies of magneto-optical properties, the possibility of elucidating the role of electrons with different spin directions (for ↓ and opposite ↑ magnetization directions) is accessible, since the magneto-optical conductivity is the difference of contributions from the electron conductances with different spin directions: co-directional with the magnetization and opposite to it [4], while the optical conductivity is the sum of these contributions.

The field of magneto-optics (MO) has been an important research topic since discovery of the Faraday and Kerr effect more than century ago. The interest in MO phenomena was prompted by these discoveries, because the effects describe the light and the substance as entities that simultaneously enclose electric and magnetic properties. A novel history of the magneto-optics phenomena has started a few decades ago in works where non-diagonal elements of optical conductivity tensor were introduced [5]. Progress in experimental techniques made it possible to perform measurements of MO spectra in a wide energy range of about 0.5 to 5 eV. Spectral ellipsometry has been always used for studying magneto-optics properties of materials as well as for developing pure practical application of the effect (*e.g.*, magnetic storage media) [6]. The Kerr spectra have been measured and calculated for numerous compounds, namely: Au-Co multilayer samples [7], Au and Mn based compounds [8] or noble metals (Cu, Ag and Au) [5]. The amount of MO experimental data at this moment has become too large and requires a detailed review. These numerous investigations resulted in a lot of evidences that experimentally obtained MO spectra can be analyzed now in frames of first-principles energy band theory.

In this study, the magneto-optical properties of Fe- and Co-based nanocomposites are studied in detail on the basis of measurements of the complex Kerr angle over a wide spectral range.

2. Theory

Components of dielectric tensor can be presented omitting the magnetic force, since they are too weak as compared to the electric forces. Dielectric susceptibility for a media $\chi_{\alpha,\beta}\,(\varepsilon_{\alpha,\beta}(\omega)=1+4\pi\chi_{\alpha,\beta}(\omega))$ can be given by [9]:

$$\chi_{\alpha,\beta}=\frac{N}{\hbar}\sum\frac{\rho_{nm}d_{nm}^{(\alpha)}d_{nm}^{(\beta)}}{\omega_{nm}-\omega-i/\tau_{nm}}, \qquad (1)$$

where $d_{nm}^{(\alpha)}$ is the dipole moment projections on the axes $\alpha=x,y,z$, τ_{nm} – lifetime parameter of ρ_{nm} non-diagonal component of the density matrix. The dipole arises as a result of optical transition between *n* and *m* energy levels. This is a basic ratio for the dielectric function without any magnetic force, though in the case of magneto-optic effects, we have to use another relationship for the resonant frequencies in Eq. (1) denominators. To do this, we have to extend classic band theory of solids considering the energy levels originated from single atom in the crystal lattice. On the one hand, it is obvious, because the properties of transition metals (*e.g.*, Fe or Co) are defined partially by incomplete *d*-shell, though technically angular quantum numbers are introduced for single atoms and do not exist in energy bands formalism. On the other hand, the theoretical approach has to be enough simple and functional in order to interpret our experimental data.

Let us take the electron gas in a metal with non-zero intrinsic magnetic field as a result of ferromagnetic spin ordering. For a simplified model of almost free electrons in the magnetic field (having kinetic energy and the coupling angular momentum to the magnetic field), their energies can be defined as:

$$E=\frac{\hbar^2k^2}{2m_e^*}-\vec{\mu}_L\vec{B}=\frac{\hbar^2k^2}{2m_e^*}-m\mu_{\rm B}B, \qquad (2)$$

where *m* is the magnetic quantum number, $2m_e^*$ – electron effective mass, μ_L – magnetic dipole moment, $\mu_{\rm B}$ – Bohr magneton. $m\mu_{\rm B}B$ member in Eq. (2) describes splitting the angular momentum $L=\frac{2m_e c}{e}\mu_L$ states, labeled by the quantum number *m*. Electrons are considered in spherical symmetry system, because our goal is to study amorphous alloys (which are spatially isotropic).

If we take an optical transition between two states, the transition frequency can be found from the following expression:

$$\omega_{ij}=-\frac{1}{\hbar}\left[E_{ij}+\frac{\hbar^2k_i^2}{2m_i^*}+\frac{\hbar^2k_j^2}{2m_j^*}-\left(m_j-m_i\right)\mu_{\rm B}B\right]. \qquad (3)$$

Here, effective masses for *i* and *j* levels are taken for holes and electrons, respectively. For MO phenomena, here we should take into account transitions that satisfy classic selection rules $\Delta l=\pm1$, $\Delta m=\pm1$, and $\Delta s=0$. For calculation of the dielectric functions, one should use Eq. (1) with the frequencies ω_{nm} defined by Eq. (3). From the pure experimental viewpoint, we should observe influences by magnetic field shift of dispersion curves along the energy axis. If we take a ferromagnetic sample, it shows a spontaneous magnetization. We can change the level of the magnetization by producing samples that are mixture of ferromagnetic and non-ferromagnetic parts.

If the electric field produces polarization that can be given applying statistical averaging

$$P=\langle ner\rangle=Tr\{\hat{\rho}ner\}. \qquad (4)$$

Let's take the wave functions in the radial symmetry approach as a product of radial and angular parts [10]:

$$\psi_{nlm}=R_{nl}(r)Y_{lm}(\theta,\varphi). \qquad (5)$$

Here, $R_{nl}(r)$ is the spherical Bessel function and $Y_{lm}(\theta,\varphi)$ is angular wave function. Similarly to hydrogen atom Schroedinger equation solutions, we can write

selection rules for coordinates based on properties of the spherical Bessel functions in Eq. (5):

$$\langle k|r_y|j\rangle = -i\Delta m\langle k|r_x|j\rangle . \qquad (6)$$

Schroedinger equation spherical harmonic solutions must be eigenfunctions both of L^2 and L_z, which are parts of Hamiltonian because of electron angular momentum and magnetic interaction. Eq. (6) defines the values of dielectric tensor components, if the media light produces polarization defined by Eq. (4) that contains the coordinate part. Here, we take transitions for circular polarized photons, where right circular photons produce transitions with $\Delta m = \pm 1$ and left circular photons with $\Delta m = -1$. Of course, the selection rules for the magnetic quantum number have to be applied simultaneously with account of the selection rules for azimuthal quantum number l: $\Delta l = \pm 1$. These transitions (which induce positive or negative helicity circular polarization (right- or left-circular polarization)) result in the non-zero non-diagonal components of dielectric tensor

$$\varepsilon_{right} = \varepsilon_{xx} - i\,\varepsilon_{xy},$$
$$\varepsilon_{left} = \varepsilon_{xx} + i\,\varepsilon_{xy}. \qquad (7)$$

The case when $\Delta l = \pm 1$ and $\Delta m = 0$ is related to the case with induced linear polarization along z coordinate.

For a ferromagnetic, magnetic field in the media is defined by spatially ordered spins. On the other hand, the direction of magnetic polarization in isotropic media can be arbitrary. If we change the spin direction (and, as a result, the magnetic field direction) to the opposite, the transitions described by Eqs (2) and (3) may be interpreted as having the opposite sign of Δm: $\Delta E = \Delta m\mu_B(-B) = (-\Delta m)\mu_B B$ or, by other words, as having the opposite sign of media polarization helicity. If $\Delta m = 0$, the energy shift $\Delta E = 0$.

Comparison of the calculated absorption spectra $\sigma(h\nu)$ in Fe–Co–B supercell with experimental data testifies that the shapes of energy bands have to be considered also from the viewpoint of selection rules both for the orbital and spin quantum numbers. In this case, the modified Spicer ratio [11] can be written as:

$$\sigma(h\nu) \cong \overline{A} \int_{E_F}^{E_F + h\nu} \rho_{l=2,\Delta s=0}(E)\rho_{l=2,\Delta s=0}(E - h\nu)dE , \qquad (8)$$

where $\overline{A}$ is the mean value of the matrix transition elements, and we calculate transitions between the states with the same spin direction $\Delta s = 0$ (spin down – spin down or spin up – spin up). Eq. (8) is a further development of our former approach described in [11].

The calculation algorithm for optical conductivity was selected as a base for development code ABINIT [12] for Linux, which is open-source software of the Universitae Catholique de Louvain project. The software allowed us to determined density of states of the super-cell with different spin orientation of Co and Fe atoms. The results of the density of states and optical conductivity calculations are presented in Figs 1 and 2.

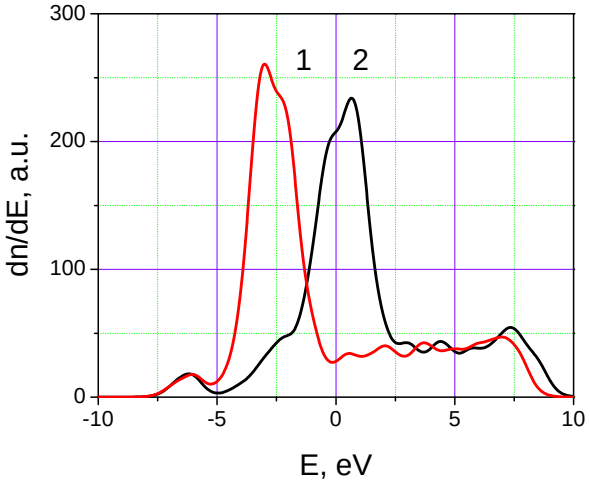

Fig. 1. Densities of electronic states for different directions of spin (*1* – spin up, *2* – spin down) for the Co_2Fe_2B superlattice. Fermi level corresponds to the energy $E_F = 0$ eV.

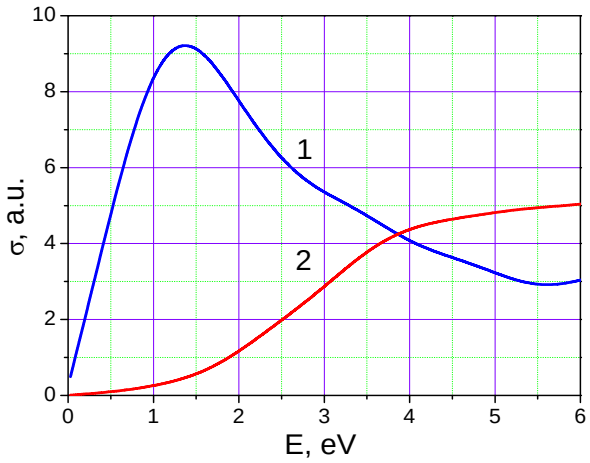

Fig. 2. Optical conductivity of the superlattice with five atoms for optical transitions taking into account the selection rules for orbital quantum number ($\Delta l = \pm 1$) and opposite orientations of spins (*1* – spin down, *2* – spin up).

The results in Fig. 1 are typical for a ferromagnetic material with lower energies for the states with spin oriented up as compared to the states with the spin oriented down. Most of the former filled states are located below Fermi level as opposite to the mostly unpopulated states related to the opposite to the intrinsic magnetic field electron spin orientation. As a result, the total spontaneous magnetization in this model is a result of drastically different numbers of the filled states with up- and down-spin orientations. Fig. 2 was obtained from Fig. 1 dependences applying Eq. (8) relationship. As we can see, the energy levels in the vicinity of 3.5 eV exhibit approximately equal contribution of electrons with different spins to the final optical conductivity dispersion curve.

3. Experimental

The samples of composite nanostructures amorphous ferromagnetic metal alloy ($Co_{41}Fe_{39}B_{20}$) – amorphous dielectric SiO_2 were fabricated using ion-beam sputtering and revealed a two-phase system: surrounded by dielectric SiO_2 matrix nanostructured granules of amorphous $Co_{41}Fe_{39}B_{20}$ alloy. The concentration x of the magnetic phase varied discretely from 19 to 56%. The sizes of the ferromagnetic particles varied from 2 to about 10 nm in dimension, increasing the content of the magnetic phase, which was chaotically distributed in the amorphous dielectric matrix SiO_2.

We carried out the measurements of magneto-optical properties inherent to amorphous nanostructures. The measurements were performed for the angles of light beam incidence 10…15 degrees. The optical behavior of anisotropic samples is described by their non-diagonal reflection Jones matrix R:

$$R = \begin{vmatrix} r_{pp} & r_{ps} \\ r_{sp} & r_{ss} \end{vmatrix}, \qquad (9)$$

p refers to the linear light polarization along the direction parallel to the plane of incidence and s refers to the linear light polarization along the direction perpendicular to the plane of incidence. r_{pp} and r_{ss} are amplitude reflection coefficients of the reflected light with p- and s-polarization, respectively. Non-diagonal amplitude coefficients r_{ps} and r_{sp} describe the changes of reflected light polarization from $p(s)$ to $s(p)$. Anisotropic reflection coefficients (r_{ps}, r_{sp}) are expected to have much lower amplitude as compared to the isotropic ones.

The complex MO Kerr angles can be defined as:

$$\theta_s + i\eta_s = r_{ps}/r_{ss},$$
$$\theta_p + i\eta_p = r_{sp}/r_{pp}, \qquad (10)$$

where $\theta_s(\theta_p)$ is the real Kerr rotation angle and $\varepsilon_s(\varepsilon_p)$ – Kerr light ellipticity. At the angles of incidence close to the normal one: $r_{ps} = -r_{sp}$ and $r_{pp} = r_{ss}$. It means that the complex Kerr effect has the form:

$$\theta_K = \theta_K + i\eta_K = r_{ps}/r_{ss}\ . \qquad (11)$$

To calculate the true and imaginary parts of the magneto-optical conductivity $\tilde{\sigma}_{xy}(h\nu) = \sigma_{xy}(h\nu) + i\sigma'_{xy}(h\nu)$, we have to know the magnitude of the optical conductivity $\tilde{\sigma}_{xx}(h\nu)$.

Non-diagonal components of optical conductivity $\tilde{\sigma}_{xy}(h\nu)$ tensor can be found from measured Eq. (11) angles applying the known relationship [5]:

$$\theta_K + i\eta_K = \frac{-\sigma_{xy}}{\sigma_{xx}\left(1 + i\frac{4\pi}{\omega}\sigma_{xx}\right)^{1/2}}. \qquad (12)$$

Spectral investigations of ellipsometric parameters for reflected light have been carried out using the spectral Woollam ellipsometer M-2000 in the wavelength range λ = 0.24…1.0 μm ($h\nu$ = 1.24…5.15 eV). The results of Kerr effect measurements are presented in Figs 3 and 4. We can evaluate resonant frequencies from Eqs (1) and (3) analyzing the curves (zero values of the real part and maximum values for the imaginary part). In Fig. 3, we can see sufficiently good resemblance between the measured and calculated curves of σ_{xy}. For example, the difference in the value of calculated and measured resonant frequency is 0.5 eV. It means the modified Spicer equation (Eq. (5)) gives us a good picture of magneto-optics effects in isotropic ferromagnetic.

4. Results and discussion

Curves from Figs 3 and 4 demonstrate shift of the resonant frequencies (zero and maximum points) as a function of ferromagnetic component concentration in the sample. The shift can be qualitatively explained based on Eq. (3) where the frequency depends on the value of magnetic field in a sample. Frequencies are higher with higher values of ferromagnetic component concentration in the samples. The effect can be subjected to ordered magnetic moments in the ferromagnetic sample which produce magnetic field there. The averaged per volume numbers of magnetic field drop for lower concentrations of ferromagnetic component resulting in lower absolute values of $(m_j - m_i)\,\mu_B B$ part from Eq. (3). As it was discussed above, the sign of $\Delta m = m_j - m_i$ determines right-handed or left-handed circular polarization of the reflected light. From this viewpoint, in Fig. 4 resonant frequencies shift to higher energies, the spectral intervals and magneto-optics Kerr effect light helicity sign are directly associated.

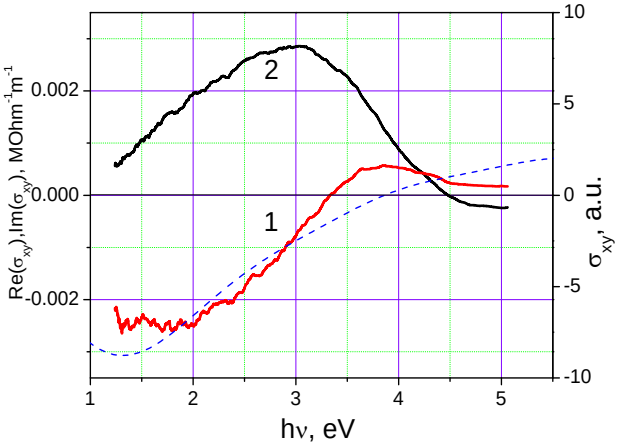

Fig. 3. Experimental curves of real (*1*) and imaginary (*2*) parts of σ_{xy} for $Co_{41}Fe_{39}B_{20}$ and the difference of calculated optical conductivity curves from Fig. 2 (dashed line).

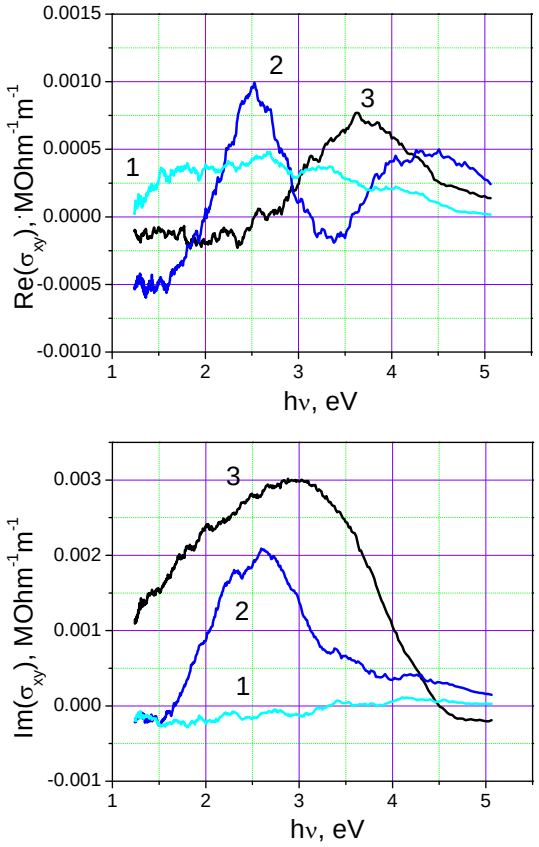

Fig. 4. Experimental curves of real and imaginary parts of σ_{xy} for $(Co_{41}Fe_{39}B_{20})_x(SiO_2)_{100-x}$ for different values of x ($1 - x = 19$, $2 - x = 33$, $3 - x = 56$).

If we have transitions from *p*- to *d*-band, theoretically we have three possible transitions for each choice of $\Delta m = \pm 1$, each term corresponds to a possible transition from an energy level with magnetic quantum number in the range $m = -1, 0, 1$ to another energy level with $m = -2, -1, 0, 1, 2$. In the case of transition metals with not fully occupied *d*-band, we can receive higher probabilities of $\Delta m = -1$ transitions (resulted in experimentally registered by us left circular polarization of the reflected light). More probable transitions correspond to $\Delta m = -1$, because of no vacancies on the level with $m = +2$ on *d*-shell for Fe (with $m = +1$ and $m = +2$ for Co). The filled levels with higher m for Fe and Co seem to be an effect of Hund's rule, where if *d*-shell is more than half-filled, the level with the highest value of $M_L + M_S$ is the lowest one in energy (M_L and M_S are the components of the total orbital angular momentum L and total spin S along the intrinsic magnetic field direction). Certainly, Hund's rule formalism should be applied for condensed matter problems as a qualitative approach. The crystal field originated from neighbouring atoms changes molecular orbitals depending on the crystal lattice symmetry [13], and we can talk about quantum number selection rules with some approximation, though in good comparison with experiments for $(Co_{41}Fe_{39}B_{20})_x(SiO_2)_{100-x}$ amorphous alloy [11].

5. Conclusions

Magneto-optics properties $(Co_{41}Fe_{39}B_{20})_x(SiO_2)_{100-x}$ have been studied both theoretically and experimentally. Our theoretical approach is based on a quantum mechanical consideration of atoms exposed to both crystal field of neighbouring atoms and to magnetic field caused by ferromagnetic ordering in the sample. The former point allows us to expand classical band theory Hamiltonian with account of electron gas coupling with intrinsic magnetic field in the vicinity of Fe and Co atoms of the alloy. Our theoretical explanation of MO effect is based on the selection rules for radial spherical Bessel functions. Also, quantum mechanical simulations of an alloy supercell allowed us to model electronic structure of the alloy and the density of states with opposite spin directions, which enabled us to evaluate off-diagonal dielectric tensor elements. In this approach, the ordered spins in the ferromagnetic totally define the intrinsic magnetic properties in the sample. Applying the modified Spicer formula for optical conductivities for different spin directions, we can obtain optical tensor off-diagonal components.

The measured dispersion curves of off-diagonal optical conductivity demonstrate shift of the resonant frequency to higher numbers for compounds with lower percentage of non-conducting SiO_2 and are in good agreement with the numerical simulation data. The shift has been qualitatively explained as the result of the magnetic field value in the sample, which defines the interaction energy between magnetic dipole and this field. The circular polarization arises in the frames of approach as a result of the transitions with specific selection rules for the magnetic quantum number as well as Hund's rule for energy levels occupation in Fe and Co atoms *d*-bands. The latter allows us to give explanation for circular polarization sign of reflected light for $(Co_{41}Fe_{39}B_{20})_x(SiO_2)_{100-x}$ alloy. The sign of non-diagonal tensor components depends on the values of magnetic quantum numbers of most probable optical transitions between the initial and final states that are populated accordingly to Hund's rule.

From the pure academic viewpoint, our approach allows us to comprehensively describe magneto-optics Kerr effect by connecting classic condensed matter band theory, quantum mechanical numerical calculus and experimental optics techniques.

Acknowledgements

The authors would like to express their deepest gratitude to Dr. V. Kravets from School of Physics and Astronomy, University of Manchester, Manchester, M13 9PL, UK for his help with spectral ellipsometric measurements.

References

1. Chang C.Z., Zhang J.S., Feng X. *et al*. Experimental observation of the quantum anomalous Hall effect in a magnetic topological insulator. *Science.* 2013. **340**. P. 167. https://doi.org/10.1126/science.1234414.

2. Dunets O.V., Kalinin Y.E., Kashirin M.A., Sitnikov A.V. Electrical and magnetic performance of multilayer structures based on $(Co_{40}Fe_{40}B_{20})_{33.9}(SiO_2)_{66.1}$ composite. *Tech. Phys.* 2013. **58**. P. 1352–1357. https://doi.org/10.1134/S1063784213090132.
3. Staschuk V.S., Kravets V.G., Lysiuk V.O., Polyanska O.P., Stukalenko V.V., Yampolsky A.L. Structure and optical properties of $(Co_{41}Fe_{39}B_{20})_x(SiO_2)_{1-x}$ nanocomposites. *Ukr. J. Phys.* 2017. **62**. P. 666–671. https://doi.org/10.15407/ujpe62.08.0666.
4. Meir Y. Transport through quantum point contacts. *Les Houches.* 2005. **81**. P. 479–493. https://doi.org/10.1016/S0924-8099(05)80051-4.
5. Uba L., Uba S., Antonov V.N. Magneto-optical Kerr spectroscopy of noble metals. *Phys. Rev. B.* 2017. **96**. P. 235392(11). https://doi.org/10.1103/Physrevb.96.235132.
6. *Developments in Data Storage: Materials Perspective*. Eds. S.N. Piramanayagam, T.C. Chong. Wiley-IEEE Press, Hoboken/Piscataway, NJ, 2011.
7. Hermann C., Kosobukin V.A., Lampel G., Peretti J., Safarov V.I., Bertrand P. Surface-enhanced magneto-optics in metallic multilayer films. *Phys. Rev. B.* 2001. **64**. P. 235422(11). https://doi.org/10.1103/Physrevb.64.235422.
8. Amft M., Oppeneer P.M. Calculated magneto-optical Kerr spectra of the half-heusler compounds AuMnX (X = In, Sn, Sb). *J. Phys. Condens. Matter.* 2007. **19**. P. 1–9. https://doi.org/10.1088/0953-8984/19/31/315216.
9. Toutounji M., Optical nonlinear response function with linear and diagonal quadratic electron-vibration coupling in mixed quantum-classical systems. *J. Chem. Phys.* 2005. **122**. P. 2228–2238. https://doi.org/10.1063/1.1864934.
10. Griffiths D.J. *Introduction to Quantum Mechanics.* Prentice Hall, Upper Saddle River, NJ, 2004.
11. Lysiuk V.O., Rozouvan S.G., Staschuk V.S. Optical properties and electronic structure of Co- and Fe-based compounds. *J. Opt. Soc. Am. B.* 2018. **35**. P. 1628–1634. https://doi.org/10.1364/Josab.35.001628.
12. Gonze X., Rignanese G.M., Verstraete M. *et al*. A brief introduction to the ABINIT software package. *Z. Kristallogr.* 2005. **220**. P. 558–562. https://doi.org/10.1524/zkri.220.5.558.65066.
13. Blundell S. *Magnetism in Condensed Matter.* Oxford University Press, New York, 2001.

Authors and CV

Viktor Lysiuk, born in 1980, received his PhD in Physics and Mathematics from the Taras Shevchenko Kyiv National University (2011) and senior scientific researcher title (2014). Senior Researcher at the Lab of Optics and Optoelectronic Registering Media, V. Lashkariov Institute of Semiconductor Physics, NAS of Ukraine. OSA Member. His research interests are ion implantation, thin films, plasmonics, ferroelectrics, and optical biosensors.

Stanislav Rozouvan, born in 1961, defended his Ph.D. thesis in optics and laser physics in 1995. Researcher at Department of Optics of the Taras Shevchenko National University of Kyiv. Authored over 70 publications, 3 patents. The area of his scientific interests includes scanning tunneling microscopy and third-order nonlinear optics.

Vasyl Staschuk, born in 1944, defended his Doctoral Dissertation in Physics and Mathematics in 2001 and became full professor in 2002. Professor of Department of Optics at the Taras Shevchenko National University of Kyiv. Authored over 150 publications, 6 patents, 5 textbooks. The area of his scientific interests includes electronic properties of disordered compounds, spectral ellipsometry of metals and thin films, optics of optoelectronic materials and devices.

Victoria Stukalenko, born in 1955, defended her Ph.D. thesis in optics and laser physics in 2005. Researcher at Department of Optics of the Taras Shevchenko National University of Kyiv. Authored 18 publications, 1 patent. The area of her scientific interests includes laser physics and Fourier optics.